Acta Pharmaceutica Sinica B 2023;13(5):2056–2070

Chinese Pharmaceutical Association
Institute of Materia Medica, Chinese Academy of Medical Sciences

Acta Pharmaceutica Sinica B

www.elsevier.com/locate/apsb
www.sciencedirect.com

ORIGINAL ARTICLE

Identification of anti-*Mycobacterium tuberculosis* agents targeting the interaction of bacterial division proteins FtsZ and SepFe

Hongjuan Zhang[a,†], Ying Chen[a,†], Yu Zhang[a], Luyao Qiao[a], Xiangyin Chi[a], Yanxing Han[a], Yuan Lin[a,*], Shuyi Si[b,*], Jiandong Jiang[a,b,*]

[a]*State Key Laboratory of Bioactive Substance and Function of Natural Medicines, Institute of Materia Medica, Chinese Academy of Medical Sciences and Peking Union Medical College, Beijing 100050, China*
[b]*Institute of Medicinal Biotechnology, Chinese Academy of Medical Sciences and Peking Union Medical College, Beijing 100050, China*

Received 26 September 2022; received in revised form 23 November 2022; accepted 8 January 2023

KEY WORDS

Anti-*Mycobacterium tuberculosis*;
FtsZ;
SepF;
Bacterial division;
Yeast two-hybrid;
CRISPRi;
Protein–protein interaction;
Inhibitor

Abstract Tuberculosis (TB) is one of the deadly diseases caused by *Mycobacterium tuberculosis* (*Mtb*), which presents a significant public health challenge. Treatment of TB relies on the combination of several anti-TB drugs to create shorter and safer regimens. Therefore, new anti-TB agents working by different mechanisms are urgently needed. FtsZ, a tubulin-like protein with GTPase activity, forms a dynamic Z-ring in cell division. Most of FtsZ inhibitors are designed to inhibit GTPase activity. In *Mtb*, the function of Z-ring is modulated by SepF, a FtsZ binding protein. The FtsZ/SepF interaction is essential for FtsZ bundling and localization at the site of division. Here, we established a yeast two-hybrid based screening system to identify inhibitors of FtsZ/SepF interaction in *M. tuberculosis*. Using this system, we found compound T0349 showing strong anti-*Mtb* activity but with low toxicity to other bacteria strains and mice. Moreover, we have demonstrated that T0349 binds specifically to SepF to block FtsZ/SepF interaction by GST pull-down, fluorescence polarization (FP), surface plasmon resonance (SPR) and CRISPRi knockdown assays. Furthermore, T0349 can inhibit bacterial cell division by inducing filamentation and abnormal septum. Our data demonstrated that FtsZ/SepF interaction is a promising anti-TB drug target for identifying agents with novel mechanisms.

*Corresponding author.
E-mail addresses: linyuan@imm.ac.cn (Yuan Lin), sisyimb@hotmail.com (Shuyi Si), jiang.jdong@163.com (Jiandong Jiang).
†These authors made equal contributions to this work.
Peer review under the responsibility of Chinese Pharmaceutical Association and Institute of Materia Medica, Chinese Academy of Medical Sciences.

https://doi.org/10.1016/j.apsb.2023.01.022

1. Introduction

Tuberculosis (TB) is one of the most prevalent infectious diseases caused by *Mycobacterium tuberculosis* (*Mtb*), which is the major leading cause of death worldwide[1,2]. In Global Tuberculosis Report 2021, about 10 million people developed TB infection in 2020, of which 1.3 million died. The End TB Strategy milestones to reduce TB disease burden were a 35% reduction of TB deaths and a 20% reduction of TB incidence rate by 2020, compared with the numbers in 2015. However, the reduction of TB death rate was only 9.2% between 2015 and 2020, nearly one quarter of the way to the milestone[3]. Furthermore, because of the COVID-19 pandemic, the global deaths from TB have increased for the first time in a decade[4]. People living with HIV and TB are more likely to experience COVID-19 infection, which remains a huge public health concern[5].

The most commonly used standard treatment for TB infection consists of four first-line drugs: isoniazid, rifampin, pyrazinamide and ethambutol. Multidrug-resistant TB (MDR-TB) was defined as TB resistant to at least isoniazid and rifampin. In Global Tuberculosis Report 2021, extensively drug-resistant TB (XDR-TB) was newly defined as the TB resistant to rifampin, any second-line anti-TB drug fluoroquinolone, and at least one of the drugs bedaquiline and linezolid[3]. Bedaquiline, together with delamanid and pretomanid are the three anti-TB drugs approved over last decade, which brought significant progress in the management of MDR and XDR-TB[6]. As expected, the resistance to three novel anti-TB drugs emerged after inadequate and frequently clinical use[7−9]. According to the WHO guidelines for anti-TB therapy, the combination of anti-TB drugs is recommended to prevent drug-resistant TB[6,10]. Therefore, more effective anti-TB agents are urgently needed to provide more options for the present therapeutic regime.

As is known, the bacterial cell division is performed by constriction of a ring-like nucleus-encoded protein complex, in which FtsZ plays a pivotal role[11]. FtsZ is a highly conserved and essential tubulin-like protein with GTPase activity[12]. It polymerizes in a GTP-dependent manner into FtsZ filaments to form the dynamic Z-ring, which provides a scaffold for recruitment of proteins needed for septum formation and cell membrane constriction[11,13]. The function of the Z-ring is modulated by these FtsZ-binding proteins that can influence its bundling, positioning and membrane interaction[14,15]. In bacteria, many of these proteins have been well characterized, such as FtsA, FtsW, SepF, ZipA, ClpX, FhaB and EzrA[16−18]. The bacterial division is significantly different from the well-understood FtsZ-based division mechanism when FtsZ-binding proteins were lacked[11,13,19]. In *Mtb*, SepF is an essential FtsZ-binding protein assists FtsZ bundling and localization at the site of division[20,21]. SepF also involves in the synthesis of peptidoglycan by interacting with MurG, an essential bacterial glycosyltransferase for new septum synthesis[20]. Both depletion and overexpression of SepF impaired the division of *Mtb*[20,22]. Several of the *Escherichia coli* and *Bacillus subtilis* FtsZ-binding proteins were absent in *Mtb*, in which SepF was found to be the alternative interaction partner[22−24]. It has been shown that FtsZ was consisted of N-terminal domain containing a nucleotide-binding pocket and C-terminal domain including a GTPase-activating site, which were connected by an α-helix (H7-helix)[25]. The C-terminal of FtsZ (363−379 amino acids) interacts with the C-terminal of SepF (115−203 amino acids), required for the interaction of FtsZ/SepF and subsequently the FtsZ filamentation and localization[20,22,26]. Therefore, the FtsZ/SepF interaction is essential for bacterial division of *Mtb* and could be a target for anti-TB agents.

In the previous study, FtsZ was considered to be an appealing target for antibacterial drugs. Plenty of synthetic small molecules, semi-synthetic compounds and natural products exhibited antibacterial activities targeting FtsZ, including *E. coli*, *B. subtilis*, *Staphylococcus aureus* and *M. tuberculosis*[27−31]. For *Mtb*, SRI-3072, totarol, zantrin, berberine and its derivatives showed anti-*Mtb* activity by inhibiting the GTPase activity of FtsZ[31,32]. In our previous studies, TB-E12 and 297 F were found as the FtsZ inhibitors of *Mtb*[33,34]. However, there were few reports of antibacterial agents targeting SepF. A natural antimicrobial compound, rhodomyrtone, displayed potent activity against *B. subtilis* targeting SepF as well as FtsA, resulting in mislocalization of the Z-ring and ultimately cell lysis[35]. Therefore, the potential for inhibitors of FtsZ/SepF interactions to be identified as the anti-TB agents remains largely unexplored.

We have developed a screening model based on the yeast-two hybrid system to identify compounds that specifically inhibit FtsZ/SepF interaction in *Mtb*. Through screening, we identified compound T0349 that inhibited this interaction and showed anti-*Mtb* activity. T0349 prohibited the promotion effect of SepF on the FtsZ polymerization, not the classical way of GTPase inhibition. GST pull-down, fluorescence polarization (FP), surface plasmon resonance (SPR) and molecular docking assays were used to detect that T0349 inhibited FtsZ/SepF interaction by binding to SepF. Consistently, T0349 exhibited increased susceptibility in *sepF* knockdown strain induced by clustered regularly interspaced short palindromic repeat (CRISPR) interference (CRISPRi) technology and the decreased susceptibility in *sepF* overexpression strain, which indicated the drug target of T0349 is likely the SepF. Moreover, T0349 significantly changed the morphology of mycobacteria by disrupting the cell division through inhibiting the formation and location of the Z-ring. All these data indicated that FtsZ/SepF interaction is an attractive target for anti-TB drug discovery that affected the bacterial cell division.

2. Materials and methods

2.1. Materials

The yeast two-hybrid system was purchased from Clontech (CA, USA). Endonucleases and *Pfu* DNA polymerase were obtained from Takara (Kyoto, Japan). Other reagents for plasmid construction were from TransGen Biotech (Beijng, China). The expression vector pET-16b(+), pET-30a(+) and pGEX4T-1 were purchased from Novagen (Darmstadt, Germany) and Amersham (Uppsala, Sweden), respectively. Antibodies against HA, c-Myc, His and GST were from Abcam (Cambridge, UK). 96-well plates and 384-well plates were purchased from Corning (New York, USA). Compound T0349 was obtained from J&K Chemical

(Beijng, China). Rifampin, isoniazid, and other reagents were from Sigma (MO, USA). Anhydrotetracycline (aTc), HADA and resazurin were purchased from MedChemExpress (Princeton, USA). CM5 sensor chip, GSTrap FF and HisTrap FF crude were from GE Health (Uppsala, Sweden). pMV261-LacZ, pRH2502 and pRH2521 were purchased from MiaoLing Plasmid Platform (Wuhan, China).

2.2. Strains

E. coli DH5α and BL21 (DE3) were from Invitrogen (Waltham, USA). *Mycobacterium smegmatis* mc^{2}155 were purchased from American Type Culture Collection (ATCC) (Rockville, USA). The bacterial strains for the MIC test were purchased from ATCC or the clinical isolates.

2.3. Plasmid construction

To construct the yeast GAL4 two-hybrid system, *ftsZ* and *sepF* genes were amplified by PCR from the genomic DNA of *M. tuberculosis* H37Rv. The PCR products were inserted into pGADT7 (activation domain, AD) and pGBKT7 (binding domain, BD) respectively, resulting the plasmids pAD-FtsZ, pAD-SepF, pBD-FtsZ and pBD-SepF. The control plasmids pAD-T, pBD-53 and pBD-lam were obtained from Clontech (CA, USA).

For the expression of FtsZ and SepF proteins in *E. coli*, *ftsZ* and *sepF* genes were cloned into pET-16b(+), pET-30a(+) and pGEX4T-1 vectors, respectively. The recombinant plasmids pET16b-FtsZ, pET30a-SepF and pGEX4T-1-FtsZ were constructed, with 6 × His tag or GST tag at the N-terminal. In the FP and SPR assay, an N-terminal truncated version of SepF (SepFc), comprising amino acids 115−203, was also constructed to pET-30(+), resulting the plasmid pET30a-SepFc with 6 × His tag at the N-terminal.

To knockdown the *ftsZ* and *sepF* genes in *M. smegmatis*, we used CRISPR interference (CRISPRi) approach. The vector pRH2502 expressing inactive *Streptococcus pyogenes dcas9* with kanamycin resistance and pHR2521 expressing sgRNA scaffold with hygromycin resistance were used. A 20-bp oligonucleotides downstream of the protospacer adjacent motif (PAM) sites against the target sequence (*ftsZ* and *sepF*) were designed as a potential specific sgRNA. The sgRNA was ligated with pHR2521. Then the recombinant pHR2521 together with pRH2502 were electroporated into *M. smegmatis* mc^{2}155. All the oligonucleotides to generate sgRNA used in this experiment are listed in Supporting Information Table S1.

The vector pMV261-LacZ was used to construct the *ftsZ* and *sepF* overexpressed plasmids. The *ftsZ* and *sepF* genes were cloned into pMV261-LacZ, generating pMV261-FtsZ and pMV261-SepF respectively. The constructed plasmids were electroporated into *M. smegmatis* mc^{2}155. The vector pMV261-LacZ was used as a control. All the successful transformants were identified by measuring β-gal activity using *o*-nitrophenyl β-D-galactopyranoside (ONPG) as the substrate.

2.4. Compound library for screening

The compound library for screening was a commercial synthetic and natural product supplied by Enamine (Kyiv, Ukraine), which was bought from J&K Chemical company (Beijng, China).

2.5. Yeast two-hybrid assay

The interaction of FtsZ and SepF protein was verified by GAL4 yeast two-hybrid system[36,37]. Plasmids pAD-FtsZ and pBD-SepF were co-transformed into yeast AH109 to generate AH109 (pAD-FtsZ + pBD-SepF). Similarly, we obtained transformants AH109 (pAD-SepF + pBD-FtsZ), AH109 (pAD-FtsZ + pBD), AH109 (pAD + pBD-SepF). Strains AH109 (pAD-T + pBD-53) and AH109 (pAD-T + pBD-lam) were used as positive or negative controls. Growth was performed on SD minimal medium (0.67% yeast nitrogen base without amino acids, 2% glucose, supplemented with appropriate nutrients). Briefly, successful transformants with above two plasmids could grow on SD/-Leu-Trp dropout plates. Fusion proteins with interactions could also grow on SD/-Leu-Trp-Ade-His plates. In addition, interactions were quantitatively measured by liquid β-gal assay with ONPG as the colored substrate. The β-gal activity was measured according to the Yeast Protocols Handbook (Clontech, USA). All the experiments were repeated three times. The protein expression in yeast was verified by Western blot using anti-HA and anti-myc antibodies.

2.6. FtsZ/SepF interaction inhibitor screening

The compound library used for this screening is a synthetic (synthesized by Enamine) products from the Institute of Medicinal Biotechnology. Yeast cells AH109 (pAD-FtsZ + pBD-SepF), AH109 (pAD-T + pBD-53) and AH109 were grown to exponential period and were diluted 100 times for screening. 198 μL of diluted cells were added into 96-well plate, and 2 μL compounds were added to the final concentration of 10 μg/mL. About 10,000 compounds were screened. Growth inhibition of yeast cells was observed after 24 h incubation at 30 °C. Meanwhile, the β-gal activity inhibition of the initial selected compounds was measured using the same method described above.

2.7. Expression and purification of recombinant proteins

Recombinant His-tagged FtsZ, His-tagged SepF, His-tagged SepFc, GST-tagged FtsZ and GST were overexpressed and purified in *E. coli* BL21 (DE3). Bacteria carrying pET16b-FtsZ, pET30a-SepF, pET30a-SepFc, pGEX4T-1-FtsZ and pGEX4T-1 were grown at 37 °C in LB medium to OD_{600} = 0.8. The expression of His-FtsZ, His-SepF, His-SepFc, GST-FtsZ and GST were induced by addition of 0.5 mmol/L isopropyl-β-D-thiogalactoside (IPTG) for 8 h at 30 °C. Subsequently, the cells were harvested and ultrasonicated. His-FtsZ, GST-FtsZ, GST and His-SepFc were expressed in supernatant, while His-SepF was found in the inclusion bodies. The inclusion bodies were washed with lysis buffer (25 mmol/L Tris-HCl, 500 mmol/L NaCl, 50 mmol/L imidazole, and 8 mol/L urea, pH 7.8). Then the supernatant of His-FtsZ, His-SepF and His-SepFc were loaded onto a Ni^{2+} His Trap chelating column. After that, the protein was eluted using a stepwise gradient of imidazole. For GST-FtsZ and GST protein, the protein supernatant was purified by affinity chromatography using prepacked columns with Glutathione Sepharose. Elution was performed with 5−10 column volumes of elution buffer (50 mmol/L Tris-HCl, 10 mmol/L reduced glutathione, pH 8.0). The denatured His-SepF protein were refolded in the buffer (25 mmol/L Tris-HCl, 50 mmol/L NaCl, 10% glycerol, 0.4 mol/L

L-arginine and 2% glycine) by dilution method at 4 °C. Finally, all the purified proteins were analyzed by SDS-PAGE followed by Coomassie blue staining. The protein concentration was measured by Brandford method.

2.8. Light scattering assay

The effect of T0349 on FtsZ assembly with SepF was monitored by a 90° light scattering assay. The enhancement of SepF on FtsZ polymerization was first detected. His-FtsZ (10 μmol/L) was mixed with different concentrations of His-SepF (0−12 μmol/L) in 25 mmol/L HEPES buffer (pH 6.5, 50 mmol/L KCl and 5 mmol/L $MgCl_2$) for 30 min. After addition of 1 mmol/L GTP, the reaction was monitored by light scattering signal at 600 nm, using a fluorescence spectrophotometer (PerkinElmer). Then, the effect of T0349 on FtsZ assembly with SepF was detected. Briefly, His-FtsZ (10 μmol/L) was incubated with T0349 (0−40 μmol/L) and His-SepF (12 μmol/L) in 25 mmol/L HEPES buffer for 30 min. Then 1 mmol/L GTP was added, and light scattering was detected described above. His-FtsZ (10 μmol/L) incubated with T0349 (0 and 40 μmol/L) were used to detect the influence of T0349 on FtsZ polymerization.

2.9. GTPase activity of FtsZ

His-FtsZ (10 μmol/L) in the presence (2 and 20 μmol/L) or absence of T0349 were incubated in the reaction buffer (50 mmol/L Tris, 5 mmol/L $MgCl_2$) at 37 °C for 30 min. Meanwhile, His-SepF (12 μmol/L) was added to each well of the above reaction, resulting the group His-FtsZ (10 μmol/L) and His-SepF (12 μmol/L) in the presence (2 and 20 μmol/L) or absence of T0349. For the control, mutFtsZ (10 μmol/L, N22A-FtsZ constructed in our lab previously) with the mutation of key amino acid in the GTPase active site of FtsZ was used[33]. Subsequently, 1 mmol/L GTP was added to the reaction buffer. The GTPase activity of FtsZ was assessed in the 96-well plate using the malachite green assay[33]. The experiments were repeated three times.

2.10. GST pulldown assay

GST, GST-FtsZ and His-SepF were expressed and purified as previously described. For the pulldown assays, GST (1.6 μmol/L) and GST-FtsZ (1.6 μmol/L) proteins were incubated with Glutathione Sepharose 4 B beads at 4 °C for 6 h, respectively. Following incubation, His-SepF (6 μmol/L) was incubated with GST and GST-FtsZ proteins at 4 °C for a further 6 h with rotation. The unbound proteins were removed by centrifugation, and the Glutathione Sepharose 4 B beads were washed three times with PBS containing 1% Triton X-100. Interactions were analyzed by Western blot using anti-GST and anti-His antibodies. Then, the effect of T0349 on FtsZ/SepF interaction was determined. The mixture of T0349 (0−20 μmol/L) and His-SepF (6 μmol/L) were added to GST-FtsZ proteins mixed with Glutathione Sepharose 4B beads for 6 h reaction. All the samples were also analyzed by Western blot using anti-GST and anti-His antibodies.

2.11. Fluorescence polarization assay

The fluorescence polarization (FP) assay was conducted in a 384-well black plate. FITC-FtsZ (FITC-SIGGDDDDVDVPPFMRR-OH, 363−379 amino acids of the full-length FtsZ) was synthesized by GenScript company (Nanjing, China). SepFc with His tag at the N-terminal was purified described above. 30 μL FITC-FtsZ (50 nmol/L) in FP buffer (10 mmol/L HEPES, 150 mmol/L NaCl, 3 mmol/L EDTA, 0.1 mmol/L NP40, pH 8.0) was incubated with different concentrations of His-SepFc (0−480 nmol/L) at room temperature for 15 min. The millipolarization unit (mP) value for FP was read using Envision Multilabel Reader (PerkinElmer). The K_d value was calculated by using one site specific binding with Hill slope equation, in which X is the logarithm of SepFc concentration, and Y is the millipolarization value. Then, different concentrations of T0349 (0.312−40 μmol/L) were incubated with SepFc (120 nmol/L) with shaking for 1 h at room temperature prior to addition of FITC-FtsZ (50 nmol/L). In addition, the reaction of FITC-FtsZ (50 nmol/L) and His-SepFc (120 nmol/L) was used as a negative control (0% inhibition), and FITC-FtsZ (50 nmol/L) only was used as a positive control (100% inhibition). FP was analyzed and the percentage inhibition of T0349 (IC_{50}) was calculated using GraphPad Prism 5.0.

2.12. Surface plasmon resonance (SPR) assay

All experiments were carried out on a Biacore T200 instrument equilibrated at 25 °C in PBS-T buffer (PBS 0.05% Tween 20 and 0.1% DMSO). CM5 sensor chip was activated using NHS/EDC amine coupling reaction. Purified His-tagged FtsZ, SepF and SepFc (115−203 amino acids of the full-length SepF) were immobilized on CM5 sensor chip in 10 mmol/L sodium acetate buffer at pH 4.5. To determine the interaction between SepF and FtsZ, FtsZ ranging from 0.08 to 20 μmol/L were injected sequentially onto the SepF immobilized surface. Meanwhile, SepF ranging from 0.08 to 10 μmol/L were injected onto the FtsZ immobilized surface. The binding of FtsZ to SepFc was also detected by injecting FtsZ (0.16−10 μmol/L) to the SepFc immobilized chip. For the binding affinity between proteins and compound, T0349 with different concentrations (1.56−100 μmol/L) were injected sequentially onto the SepF, FtsZ and SepFc immobilized surfaces. The equilibrium dissociation constant (K_D) was analyzed by fitting the dose−response curve using BIAcore evaluation software.

2.13. RNA extraction and RT-qPCR

CRISPRi-mediated knockdown strains were cultured to OD_{600} between 0.1 and 0.2 and induced by aTc (0−200 ng/mL) for 12 or 48 h. The cells were harvested by centrifugation and re-suspended in 200 μL lysozyme (10 mg/mL) at 37 °C for 30 min. After adding 1 mL TRI Reagent, the cells were mechanically disrupted with 0.1 mm Zirconia beads by agitating the samples 6−10 times at 70 Hz for 45 s at intervals of 60 s. Total RNA was extracted as previously described[38]. RNA purification was carried out according to the manufacturer instructions (Invitrogen, USA). Finally, RNA was treated with the TURBO DNA-free Kit (Thermo Fisher, USA) to remove traces of contaminating DNA. The quantity of RNA was determined by measuring OD_{260}/OD_{280}.

In order to quantify the expression of *dcas9*, *ftsZ* and *sepF*, reverse transcription (RT) and qPCR were performed using HiFiScript cDNA Synthesis Kit and UltraSYBR Mixture (CWBIO, China). Breifly, cDNA was synthesized from 100 ng RNA. qPCR was performed with 2 μL cDNA of either *sigA* primers or *ftsZ* and *sepF* primers listed in Table S1. Samples were run on ABI 7500 Fast real-time PCR equipment at 95 °C for

10 min, following by 40 cycles of 95 °C for 15 s and 60 °C for 1 min. The mRNA levels of *dcas9*, *ftsZ* and *sepF* were normalized against the mRNA of the reference gene *sigA*.

2.14. T0349 susceptibility determination using CRISPRi-mediated knockdown strains

M. smegmatis mc^{2}155 knockdown strains expressing *dcas9* and sgRNA targeting *ftsZ* or *sepF* were tested for susceptibility to T0349. The cells were grown to an OD_{600} between 0.1 and 0.2 in 7H9 medium, followed by induced with an aTc of 200 ng/mL for 6 h. After that, cultures were diluted to an OD_{600} of 0.05. 100 μL diluted cells with 200 ng/mL aTc were mixed with a series of T0349 (0−4 μg/mL) in 96-well plate and incubated at 37 °C for 24 h. After incubation, 30 μL of 0.2 mg/mL resazurin was added for another 12 h at 37 °C. At last, the plate was read in fluorescent plate reader (Ex 560 nm/Em 590 nm). Fluorescence (%) was defined as the fluorescent value compared to control wells with no T0349.

2.15. T0349 susceptibility determination in M. smegmatis overexpression strains

The *M. smegmatis* strains for overexpression of *ftsZ* or *sepF* were cultured in 7H9 medium to OD_{600} of 0.6−0.8, respectively. The diluted cultures (OD_{600} = 0.05) were mixed with T0349 (0−4 μg/mL) in the 96-well plate and incubated for 24 h. Finally, resazurin was added to detect the susceptibility of T0349 as described above.

2.16. Molecular docking

The structure of *Mtb* SepF was predicted using SWISS-MODEL. Molecular docking of T0349 with SepF was analyzed using Discovery Studio 2018R2 by C-DOCKER program. The active center of SepF was defined as receptor cavity in the interacting domain with FtsZ (115−203 aa of SepF)[20,22]. According to the energy score and binding type, the binding mode and key amino acids were analyzed.

2.17. Fluorescence microscopy analysis

For imaging, *M. smegmatis* were grown in 7H9 medium to an OD_{600} of 0.2. T0349 (2 μg/mL) was added in the culture for another 2.5 h at 37 °C. For HADA labeling, cultures were incubated with HADA (0.5 mmol/L) for 20 min at 37 °C in dark. Finally, cells were fixed on the 1% agarose pads to be visualized using Leica DM2500 microscope with a Leica DFC450C camera under magnification. Different visual fields were examined. The length of the cells was measured by ImageJ software.

2.18. Anti-Mtb and anti-bacterial activity

The anti-*Mtb* activity of T0349 was determined by a Microplate Alamar Blue assay (MABA) method[39]. Standard *M. tuberculosis* strain H37Rv, clinically sensitive strains STB-FJ05349 and STB-FJ05060, drug resistant clinical isolates MDR-FJ05120 MDR-FJ05189 and XDR-FJ05195 were examined in the assay. Rifampin and isoniazid were used as reference drugs. The concentrations of each compound tested ranged from 0.125 to 256 μg/mL by two-fold dilution. The MIC was determined as the lowest drug concentration preventing a color change from blue to pink.

The anti-bacterial activity of T0349 was also assessed using the agar dilution method described in the Clinical and Laboratory Standards Institute (CLSI)[40]. Various bacteria (including ATCC and clinical strains) were examined in the assay. Levofloxacin was used as the reference. The MIC was defined as the lowest drug concentration inhibiting the visible growth of the bacteria after incubation.

2.19. Animal toxicity analysis

ICR mice (18−22 g, male: female = 1:1) were obtained from Vital River Laboratories and divided randomly into four groups (n = 10). Animals were orally administrated T0349 at three single doses of 100, 250 and 500 mg/kg. Saline group was used as a control. Mice survival and changes in body weight were monitored for 7 days. The animal experiments were approved by the Laboratories' Institutional Animal Care and Use Committee of the Chinese Academy of Medical Sciences (Beijing, China), with the ethical approval number 00009057.

2.20. Statistical analysis

Statistical analysis was conducted by using GraphPad Prism 8.0 software (San Diego, CA, USA). Data are presented as mean ± standard deviation (SD) based on three independent experiments. Statistical differences were assessed by one-way ANOVA followed by Tukey's multiple comparison tests.

3. Results

3.1. The interaction of FtsZ/SepF detected by yeast two-hybrid

The crystal structure and biological analysis have revealed that FtsZ and SepF interact with each other in the bacterial cell division[41]. In order to identify compounds that inhibit *M. tuberculosis* FtsZ/SepF interaction, we used yeast two-hybrid system that was applied to screen anti-TB agents targeting L12/L10 interaction in our previous study[37]. For this purpose, we constructed yeast cells AH109 (pAD-FtsZ + pBD-SepF) and AH109 (pAD-SepF + pBD-FtsZ), in which *M. tuberculosis ftsZ* and *sepF* genes were fused with GAL4 activating and binding domains, respectively. The interaction of FtsZ and SepF could bring the GAL4 activating and the binding domain together to form a complete GAL4 transcription factor, leading the reporter genes *ADE2*, *HIS3* and *LacZ* activated. Thus, the interaction between FtsZ and SepF could be detected depending on the growth of yeast cells on the SD/-Leu-Trp-Ade-His plates, or the β-gal activity using ONPG as colored substrates (Fig. 1A).

As is shown in Fig. 1B and C, yeast cells AH109 (pAD-FtsZ + pBD-SepF) and AH109 (pAD-SepF + pBD-FtsZ) grew well on SD/-Leu-Trp-Ade-His plates and was positive for β-gal activity as well. The positive control AH109 (pAD-T + pBD-53) produced the same results. As a negative control, AH109 (pAD-T + pBD-lam) did not show growth. In addition, yeast cells expressing pAD-FtsZ or pBD-SepF alone did not grow on SD/-Leu-Trp-Ade-His plates and showed negative β-gal activity, indicating the exclusion of self-activation. Moreover, we used Western blot to validate the expression of proteins FtsZ and SepF in yeast cells (Fig. 1D). These results indicate that *M. tuberculosis* FtsZ and SepF interacted with each other, and this interaction was confirmed by yeast two-hybrid system.

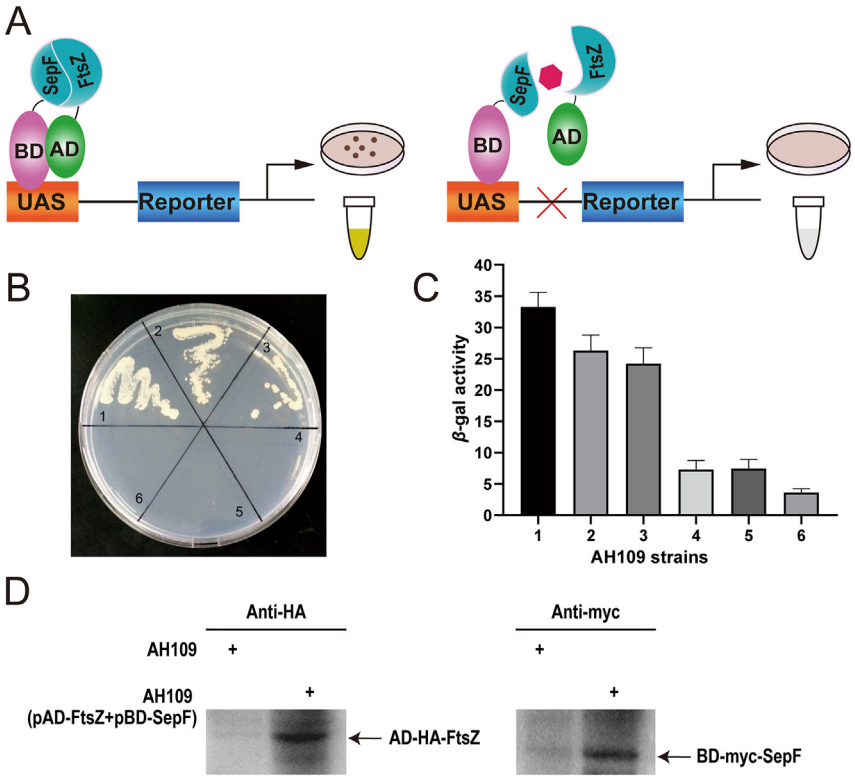

Figure 1 A yeast two-hybrid assay to detect the FtsZ/SepF protein interaction. (A) Schematic for the high-throughput screening using the yeast two-hybrid system. The function of the Gal4 protein was reconstituted by FtsZ/SepF interaction, resulting in the expression of reporter genes, *ADE2*, *HIS3* and *LacZ*. The yeast cells grew in the SD/-Leu-Trp-Ade-His dropout medium and the β-gal activity showed yellow using ONPG as the substrate (left). Compounds that blocked FtsZ/SepF interaction prevented the growth of yeast cells in SD/-Leu-Trp-Ade-His dropout medium and inhibited the β-gal activity (right). (B) Growth of AH109 strains with indicated plasmids on a SD/-Leu-Trp-Ade-His dropout plate. 1, AH109 (pAD-T + pBD-53); 2, AH109 (pAD-FtsZ + pBD-SepF); 3, AH109 (pAD-SepF + pBD-FtsZ); 4, AH109 (pAD-FtsZ + pBD); 5, AH109 (pAD + pBD-SepF); 6, AH109 (pAD-T + pBD-lam). (C) Quantification of β-gal activity in AH109 strains using ONPG as the substrate. 1−6 represented the AH109 stains with the same indicated plasmids in (B) ($n = 3$), data shown are mean value ± SD. (D) Expression of FtsZ and SepF proteins in yeast cells using anti-HA and anti-myc antibodies.

3.2. *Drug screening for FtsZ/SepF interaction inhibitors*

To screen for *M. tuberculosis* FtsZ/SepF interaction inhibitors, yeast cells AH109 (pAD-FtsZ + pBD-SepF) was used. AH109 (pAD-FtsZ + pBD-SepF) in SD/-Leu-Trp-Ade-His medium was analyzed in 96-well plate in the presence of various compounds of 10 μg/mL. About 10,000 compounds from a commercial synthetic and natural product supplied by Enamine were screened, and 38 compounds of them inhibited the growth of AH109 (pAD-FtsZ + pBD-SepF) in SD/-Leu-Trp-Ade-His medium at 10 μg/mL. Yeast cells AH109 (pAD-T + pBD-53) in SD/-Leu-Trp-Ade-His medium were used to exclude the possibility that positive compounds disrupt the GAL4 expression system (3 compounds excluded). Meanwhile, yeast cells AH109 in YPD medium were also used to exclude the possibility that the selected compounds were the antifungal ones (another 27 compounds excluded). From the initial screening, 8 typical FtsZ/SepF interaction inhibitors were selected, which inhibit the growth of AH109 (pAD-FtsZ + pBD-SepF) in SD/-Leu-Trp-Ade-His medium, leaving the growth of AH109 (pAD-T + pBD-53) in SD/-Leu-Trp-Ade-His medium and AH109 in YPD medium unaffected (Fig. 2A). For further identification, 8 initial positive compounds were subjected to β-gal activity assay. Different concentrations of compounds were added to yeast AH109 (pAD-FtsZ + pBD-SepF), and subsequently conducted β-gal activity using ONPG as substrate (Supporting Information Fig. S1). Among these selected compounds, T0349 showed a clear β-gal inhibition of yeast AH109 (pAD-FtsZ + pBD-SepF) at 2 μmol/L, and an almost completely inhibition at 16 μmol/L, while leaving yeast AH109 (pAD-T + pBD-53) unaffected (Fig. 2C). Moreover, T0349 inhibited the β-gal activity of yeast AH109 (pAD-FtsZ + pBD-SepF) in a dose-dependent manner. Therefore, T0349 was selected as the candidate for further study. The structure of T0349 (1-{4-[2-hydroxy-3-(naphthalen-2-yloxy) propyl]-1,4-diazepan-1-yl}-3-(naphthalen-2-yloxy) propan-2-ol) was shown (Fig. 2B).

3.3. *T0349 inhibited the promotion effect of SepF on FtsZ assembly*

It has been previously shown that SepF could increase the assembly of FtsZ to form FtsZ polymers[42,43]. To assess the effects of T0349 on FtsZ assembly with SepF, light scattering technology was used. FtsZ and SepF proteins with His-tag at the N-terminal were purified, respectively (Supporting Information Fig. S2A and S2B). First, the effect of SepF on FtsZ polymerization was detected. As is shown in Fig. 2D, SepF increased the light scattering intensity of FtsZ polymerization in a dose-dependent

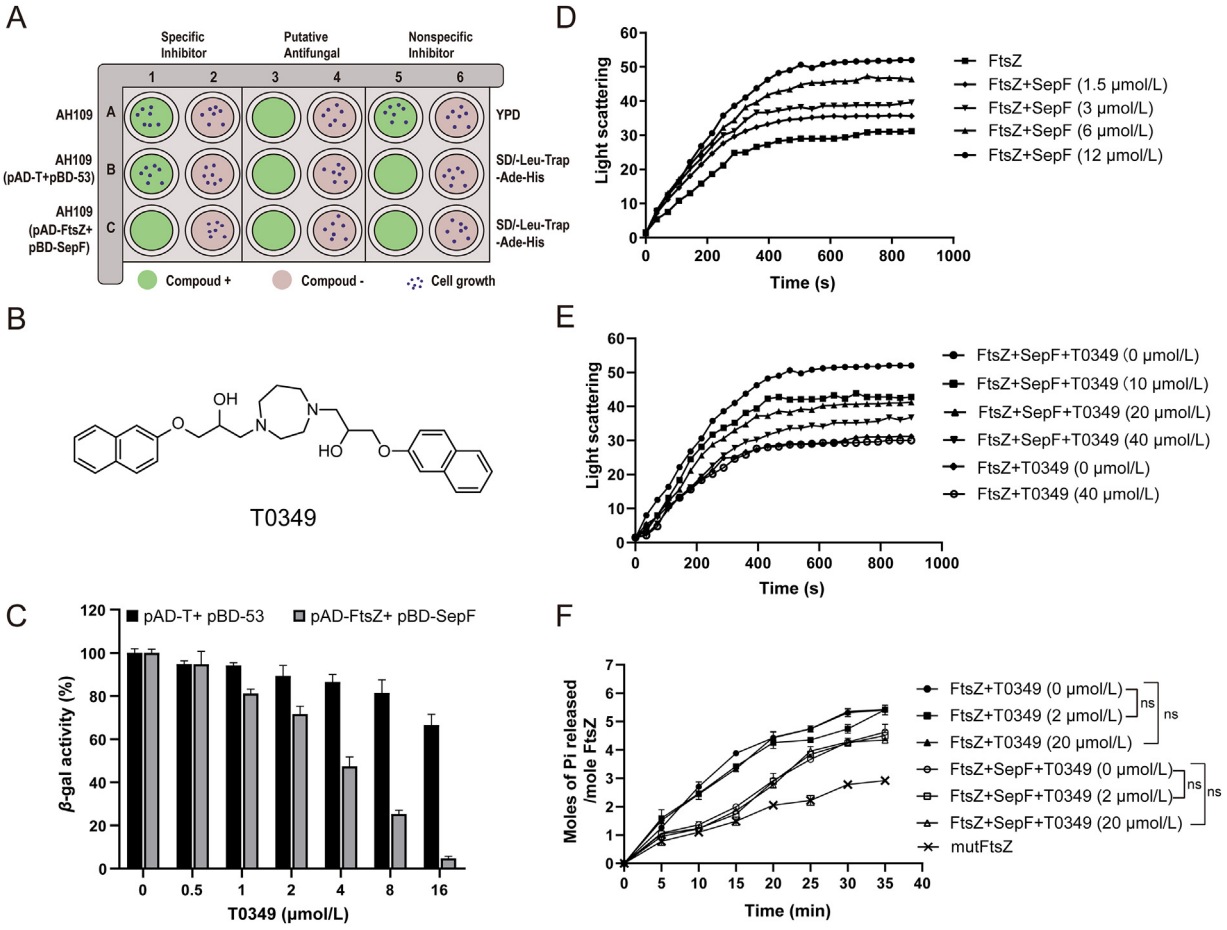

Figure 2 Identification of compounds that blocked the FtsZ/SepF interaction. (A) The strategy to screen compounds with growth inhibition of yeast cells. AH109 strains with indicated plasmids were inoculated in SD/-Leu-Trp-Ade-His dropout medium with or without compound in 96-well plates (Middle and Bottom). AH109 inoculated in YPD medium with or without compound were also used as controls (Top). (B) Structure of compound T0349. (C) Inhibition of β-gal activity of AH109 (pAD-FtsZ + pBD-SepF) cells by T0349 at indicated concentrations (0−16 μmol/L). Strain AH109 (pAD-T + pBD-53) was used as a control. Values represent the ratio of β-gal activity in cells treated with T0349 over that in untreated cells. (D) FtsZ polymerization in the presence of various concentrations of SepF (0−12 μmol/L). (E) The effect of T0349 on FtsZ polymerization with SepF. FtsZ (10 μmol/L) and SepF (12 μmol/L) were mixed with different concentrations of T0349 (0−40 μmol/L). FtsZ (10 μmol/L) with T0349 (40 μmol/L) was used as a control to exclude the effect of T0349 on FtsZ polymerization. (F) The effect of T0349 on GTPase activity of FtsZ. T0349 with indicated concentrations (0−20 μmol/L) were incubated with FtsZ in the absence or presence of SepF. mutFtsZ (N22A-FtsZ) was used as a negative control. The amount of released Pi from GTP catalyzed by FtsZ was detected using malachite green assay at 650 nm. Data shown are mean value ± SD, $n = 3$. ns means not significant.

manner. The light scattering intensity increased by almost 15%, 30%, 50%, 70% in the presence of 1.5, 3, 6 and 12 μmol/L SepF, compared with the control (without SepF). On addition of T0349, the enhancement effects of SepF on FtsZ polymerization were impaired. T0349 (10, 20 and 40 μmol/L) reduced the light scattering intensity of FtsZ assembly with SepF by 20%−40%, compared with the control (without T0349) (Fig. 2E). It has been shown that the light scattering intensity of FtsZ polymerization remained the same with or without T0349 (40 μmol/L), which means that T0349 alone could not inhibit FtsZ polymerization (Fig. 2E).

As the assembly of FtsZ depends on both the interaction of FtsZ/SepF and the GTPase of FtsZ, we further examined the effect of T0349 on GTPase activity of FtsZ. Fig. 2F shows that a mutation in GTPase active site of FtsZ (mutFtsZ) reduced the GTPase activity. Alternatively, there was no statistically significant difference between the groups with or without T0349. Thus, T0349 (2 and 20 μmol/L) did not inhibit the GTPase activity of FtsZ with or without SepF. These data demonstrate that T0349 reduced the FtsZ assembly with SepF, not by inhibiting the GTPase activity of FtsZ.

3.4. *T0349 disrupted the interaction of FtsZ/SepF*

As the interaction of SepF and FtsZ promotes the FtsZ polymerization, we speculated that T0349 disrupted the interaction of FtsZ/SepF. To determine whether T0349 abolished FtsZ/SepF interaction, GST pull-down assay, fluorescence polarization (FP) and surface plasmon resonance (SPR) techniques were used.

The disruption of FtsZ/SepF interaction by T0349 was examined by GST pull-down assay, which is widely used to

examine protein−protein interaction *in vitro*. First, GST-FtsZ and GST were successfully purified in *E. coli* (Fig. S2C and S2D). The interaction between FtsZ and SepF was confirmed using GST-FtsZ as a bait. Western blot analysis using anti-His antibody showed that His-SepF was detected with GST-FtsZ, which was absent with GST as a bait (Fig. 3A). This indicated a strong interaction of FtsZ/SepF. To determine the inhibitory effect of T0349, immobilized GST-FtsZ (bait) and His-SepF were incubated with T0349 at indicated concentrations. The levels of GST-FtsZ and His-SepF in the resulting pull-down products were analyzed by Western blot assay. Interestingly, the presence of T0349 significantly reduced the level of His-SepF in the pull-down products in a dose-dependent manner, leaving GST-FtsZ unaffected (Fig. 3B).

FP assay has also been widely used to analyze protein−protein interactions. For a fluorescent peptide/protein, the interaction of a peptide/protein can be detected through the increase of mP values when the interaction complex formation occurs[44]. In this assay, we first synthesized a peptide FITC-FtsZ, with FITC-labeling on the N-terminus of 363−379 amino acids of the full-length FtsZ, the critical interacting parts of SepF. SepFc (115−203 amino acids of the C-terminal SepF) which was considered as the interacting parts with FtsZ, was also purified in *E. coli* with His tag on the N-terminal (Fig. S2E). 50 nmol/L FITC-FtsZ was used as the probe. As illustrated in Fig. 3C, the mP values increased in a dose-dependent manner when His-SepFc was incubated, reaching a plateau at 120 nmol/L His-SepFc, with a K_d value of 18.57 nmol/L. To identify the inhibitory effect of T0349, 50 nmol/L FITC-FtsZ and 120 nmol/L His-SepFc were selected. T0349 showed a dose-dependent inhibition against FITC-FtsZ/His-SepFc interaction with an IC_{50} of 20.42 μmol/L (Fig. 3D).

Based on the result that T0349 significantly inhibited the interaction of FtsZ/SepF in GST pull-down and FP assay, FtsZ or SepF might be the possible binding target of T0349. Therefore, we detected the binding of T0349 to FtsZ and SepF by SPR technique, which was widely used for quantitatively measuring intermolecular interactions[45]. First, His-FtsZ and His-SepF were coated on the CM5 sensor chip respectively. The SepF immobilized sensor chip was exposed to various concentrations of FtsZ (0.08−20 μmol/L). FtsZ was able to bind with SepF in a dose-dependent manner, indicated by a measurable change in response units (RUs) (Fig. 4A). Similarly, SepF could bind with FtsZ observed in the FtsZ immobilized sensor chip (Fig. 4B). The K_D value for FtsZ/SepF interaction was 1.13 μmol/L. When His-SepFc was immobilized, the K_D value for the SepFc/FtsZ

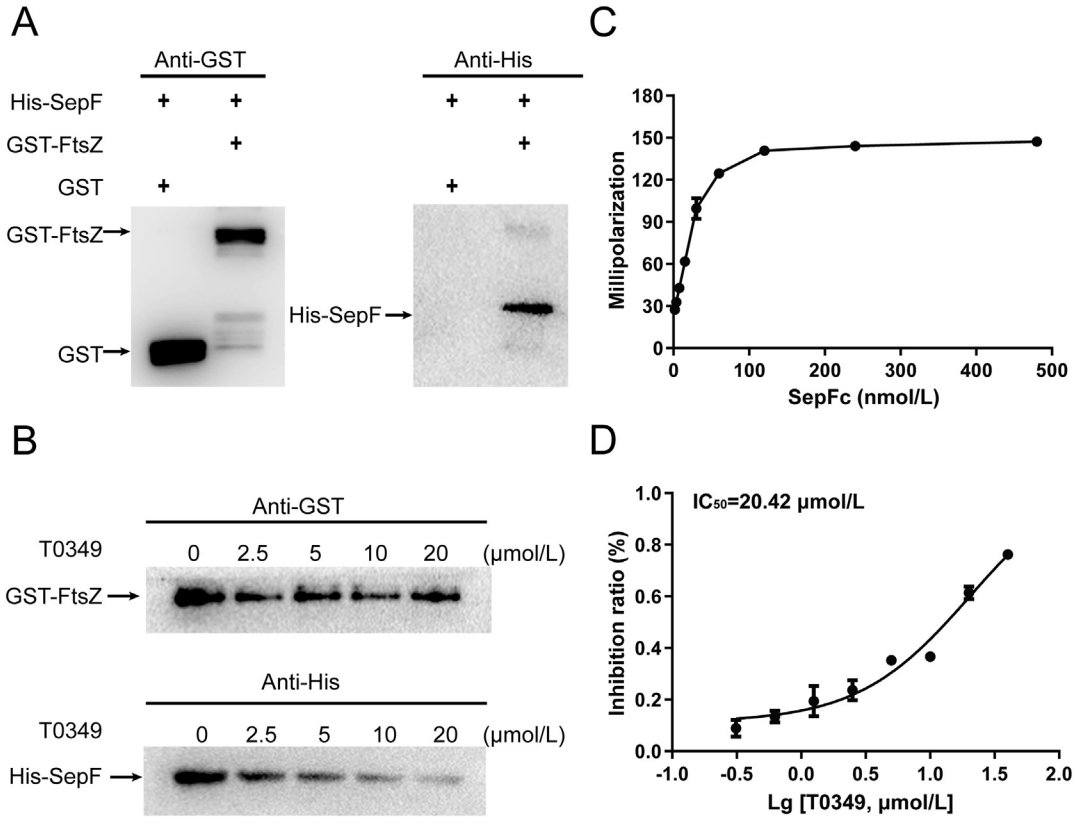

Figure 3 Disruption of the interaction between FtsZ and SepF by T0349. (A) Identification of FtsZ/SepF interaction by GST pull-down assay. Purified GST-FtsZ (1.6 μmol/L) or GST (1.6 μmol/L) were immobilized on Glutathione-Sepharose 4 B beads, followed by incubated with His-SepF (6 μmol/L). The samples were detected by Western blot with anti-GST and anti-His antibodies. (B) T0349 blocked the FtsZ/SepF interaction. Different concentrations of T0349 (0−20 μmol/L) and His-SepF were together added to Glutathione-Sepharose 4 B beads bound with GST-FtsZ proteins. All the samples were verified by Western blot with anti-GST and anti-His antibodies. (C) The binding of FtsZ and SepF detected by FP. FITC-FtsZ (50 nmol/L) was incubated with 0−480 nmol/L His-SepFc, of which the binding was indicated by the millipolarization value. K_d = 18.57 nmol/L. (D) The inhibition of FtsZ/SepF interaction by T0349 detected by FP. SepFc (120 nmol/L) incubated with T0349 (0.312−40 μmol/L) were added to FITC-FtsZ. The IC_{50} was calculated as the inhibition ratio of the millipolarization values over the concentration of T0349 that fitted to a variable-slope dose−response equation. IC_{50} = 20.42 μmol/L. Data shown are mean value ± SD, n = 3.

interaction was 5.16 μmol/L, a value that in the same range as the K_D value for SepF/FtsZ interaction (Fig. 4C). To determine whether T0349 bind to FtsZ and SepF, we exposed T0349 to FtsZ and SepF immobilized sensor chip respectively. Interestingly, T0349 bound to SepF immobilized sensor chip as evidenced by the changes in RUs with the K_D of 47.7 μmol/L (Fig. 4D). However, T0349 failed to bind to FtsZ (Fig. 4E). As is shown in Fig. 4C, the interaction of SepFc with FtsZ was identified. To further detect the binding mechanism, T0349 was exposed to SepFc immobilized sensor chip. As expected, T0349 was able to bind to SepFc with the K_D of 46.75 μmol/L, suggesting that T0349 could bind with the interacting part of FtsZ/SepF (Fig. 4F). All these data collectively demonstrate that T0349 inhibited FtsZ/SepF interaction by binding with SepFc.

3.5. *Susceptibility determination of T0349 in ftsZ or sepF knockdown and overexpression strains*

CRISPR interference (CRISPRi) technology has been recently developed to identify essential genes for the novel drug targets[46]. It introduces a new way to repress sequence specific genes by coexpressing a catalytically inactive Cas9 (*dcas9*) and single guide RNA (sgRNA)[47]. To examine the drug target of T0349, we constructed the CRISPRi-mediated *ftsZ* or *sepF* knockdown strains.

In this research, we used an anhydrotetracycline (aTc)-inducible *dcas9* expression system, in which *dcas9* was expressed under the control of aTc. The sgRNA binds to the target gene and recruits dCas9 to the site to lower levels of RNA of the target gene. First, we evaluated the efficiency of CRISPRi system in *M. smegmatis*, a strain close to *M. tuberculosis* with nonpathogenic and fast-growing. The sgRNAs were designed targeting the specific sequence of *ftsZ* or *sepF* (Table S1). Expressions of *dcas9*, *ftsZ* and *sepF* in the CRISPRi-mediated knockdown strains were determined by RT-qPCR at 12 h after addition of different concentrations of aTc (0−200 ng/mL). As is shown in Fig. 5A and C, expression of *dcas9* was gradually increased by up to 500-fold after treating with ≥50 ng/mL of aTc. In contrast, the expression of *ftsZ* was reduced by 50%, 91%, 94%, 98%, 99% and 99% treated with 1, 4, 10, 50, 100 and 200 ng/mL aTc, in comparison with the mRNA levels in the untreated *M. smegmatis* (Fig. 5A). Similar results were observed in the *sepF* target CRISPRi-mediated knockdown strains (Fig. 5C). The results demonstrate that expressions of *ftsZ* and *sepF* gene were suppressed by at least 90% with ≥4 ng/mL aTc for 12 h. Next, we detected the stability of this CRISPRi system. The expression of *dcas9*, together with its repressions to *ftsZ* and *sepF* genes were examined in presence of 50 and 200 ng/mL aTc over a period of 48 h. We observed ~500-fold induced expression of *dcas9* at 12 h after addition of 50 and 200 ng/mL aTc, followed by a stable expression at 24, 36 and 48 h. In contrast, the expression of *ftsZ* exhibited a 90% reduction relative to the uninduced control at 12 h with 50 ng/mL aTc, decreasing to 10% reduction at 48 h (Fig. 5B). While for the 200 ng/mL aTc group, the reduction of *ftsZ* could still achieve 80% at 48 h. Similar results were obtained in the CRISPRi-mediated *sepF* knockdown strains (Fig. 5D). Therefore, 200 ng/mL aTc was used to induce the *ftsZ* or *sepF* knockdown strains for susceptibility analysis of T0349. The morphology of *ftsZ* or *sepF* knockdown *M. smegmatis* strains were shown in Supporting Information Fig. S3.

Next, we determined whether knockdown of *ftsZ or sepF* resulted in increased susceptibility to T0349. The resazurin assay, indicated by the fluorescent value, was used for its convenient and accurate evaluation of cellular growth and viability[48]. Treated with the same concentration of T0349 (0−4 μg/mL), the viability of the *sepF* knockdown strain significantly reduced than the wildtype strain (vector control) (Fig. 5E). While for the *ftsZ* knockdown strain, the viability was almost the same with the wild type (vector

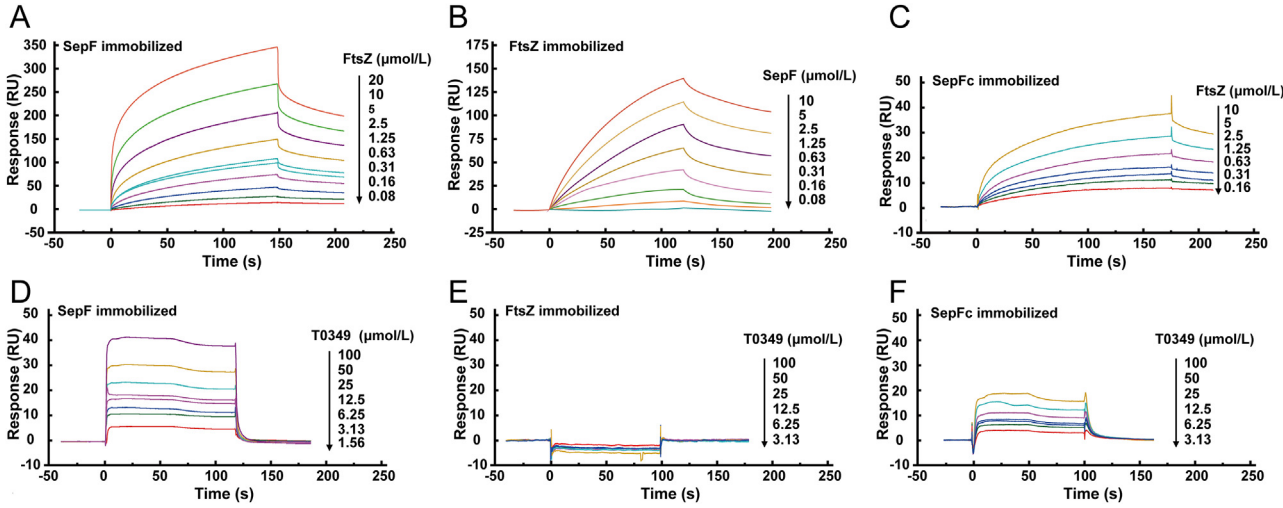

Figure 4 SPR analysis for binding of T0349 to FtsZ and SepF proteins. (A) Detection of FtsZ/SepF interaction using SepF immobilized sensor chip. Various concentrations (0.08−20 μmol/L) of purified FtsZ were injected into the chamber. (B) Demonstration of FtsZ/SepF interaction. Various concentrations (0.08−10 μmol/L) of purified SepF were injected into the FtsZ immobilized sensor chip. (C) To detect FtsZ/SepFc interaction, various concentrations (0.16−10 μmol/L) of purified FtsZ were injected into SepFc immobilized sensor chip. (D) Binding of T0349 to SepF. A sensor chip coated with purified SepF was exposed to T0349 ranging from 1.56 to 100 μmol/L. (E) Binding of T0349 to FtsZ. Various concentrations (3.13−100 μmol/L) of T0349 were injected into the FtsZ coated chip. (F) Binding of T0349 to SepFc. T0349 (3.13−100 μmol/L) were injected into the SepFc immobilized chip. The change in response units was shown over time. The K_D was determined using BIAcore evaluation software.

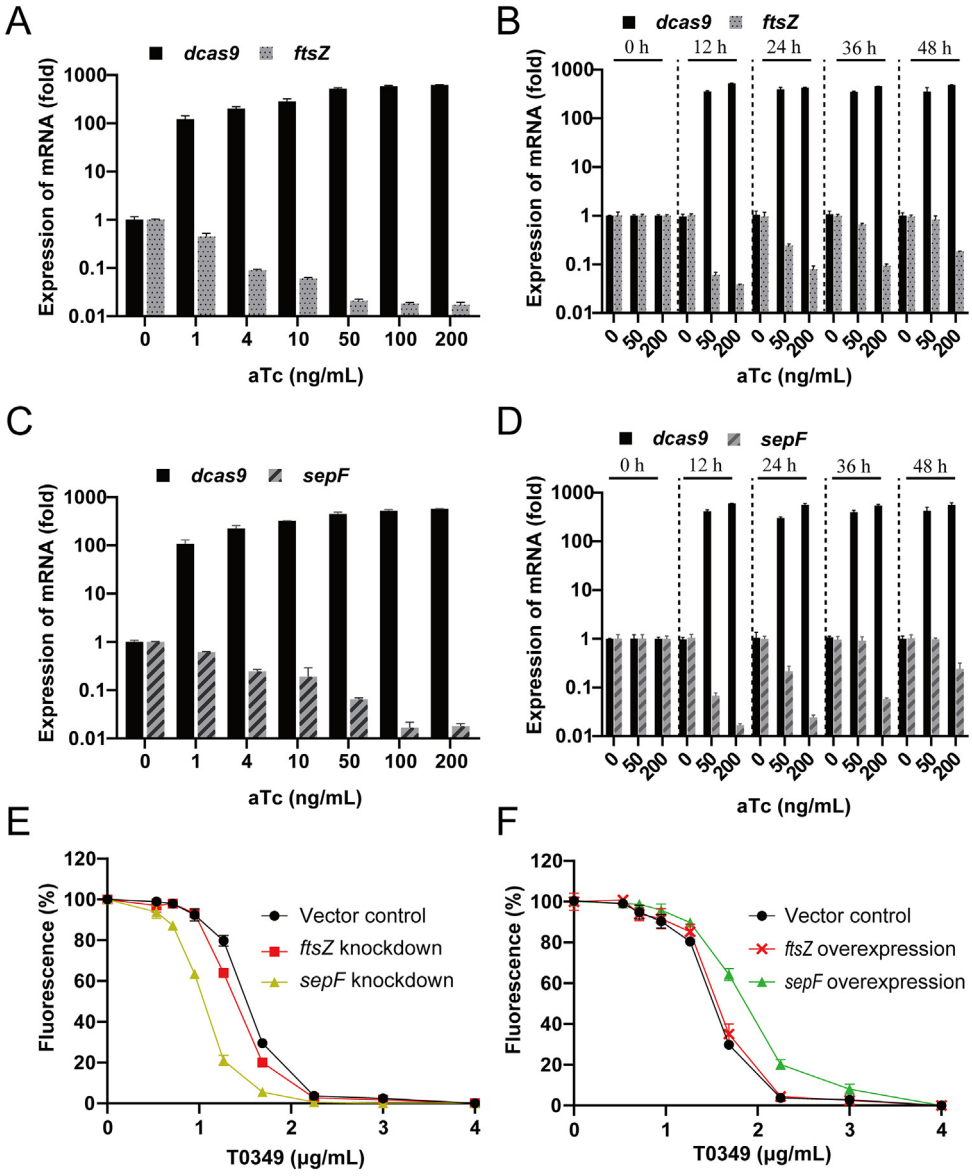

Figure 5 The susceptibility analysis of T0349 in *ftsZ* or *sepF* knockdown and overexpression strains. (A, B) Knockdown of *ftsZ* by CRISPRi in *M. smegmatis*. Expression of *dcas9* and *ftsZ* in the aTc-inducible knockdown *M. smegmatis* strain with indicated concentrations (0−200 ng/mL) of aTc treatment (A) and over a period of 48 h (B). Expression was determined by quantitative real-time PCR. (C, D) Knockdown of *sepF* by CRISPRi in *M. smegmatis*. (E) The susceptibility analysis of T0349 in *ftsZ* or *sepF* knockdown *M. smegmatis* strain. The growth and viability of the strain indicated by the fluorescence were shown with different concentrations of T0349 (0−4 μg/mL). (F) The susceptibility analysis of T0349 in *ftsZ* or *sepF* overexpression *M. smegmatis* strain. Data shown are mean value ± SD, $n = 3$.

control). Thus, the susceptibility of *sepF* knockdown strain to T0349 was increased, which suggested that SepF might be the target of T0349.

To further investigate the drug target of T0349, we constructed *ftsZ* and *sepF* overexpression plasmids, pMV261-FtsZ and pMV261-SepF respectively. These plasmids were introduced into *M. smegmatis* and confirmed by measuring β-gal activity using ONPG as substrate (Supporting Information Fig. S4). As is shown, the viability of *sepF* overexpression strain distinctly increased compared with the wild type (vector control) treated with the same concentration of T0349 (Fig. 5F). However, the viability of the *ftsZ* overexpression strain maintained almost the same. The susceptibility of *sepF* overexpression strain to T0349 was decreased. Therefore, the susceptibility analysis to both knockdown and overexpression strains verified that SepF was likely the target of T0349.

3.6. *Molecular docking between T0349 and SepF*

To detect the binding mode of T0349 with SepF, molecular docking was performed. The results giving the highest score for −CDOCKER energy and −CDOCKER interaction energy indicated the most possible docking mode of T0349 and the active center of SepF. The hydrogen atom of hydroxyl in T0349 formed conventional hydrogen bonds (H-bond) with oxygen atom of D194. One naphthyl of T0349 formed pi−alkyl interaction with

both A189 and K190, while the other naphthyl formed amide−pi stacked with A197 (Supporting Information Fig. S5A, S5B). Based on this molecular docking model, T0349 occupied the interaction domain of SepF and FtsZ in the active pocket of SepF. Therefore, it might be able to block the interaction of SepF and FtsZ by binding with SepF.

3.7. *The effect of T0349 on M. smegmatis morphology*

To examine the effect of T0349 on division of *M. tuberculosis*, we used *M. smegmatis*, a strain close to *M. tuberculosis* with nonpathogenic and fast-growing. As T0349 inhibited FtsZ/SepF interaction, we speculated that it could induce strain filamentation and abnormal septum. HADA is a fluorescent D-amino acid, which is suitable for labeling peptidoglycan in live bacteria[49]. As the Z-ring provides the energy for membrane constriction and guides the synthesis of septal peptidoglycan, HADA could be used as an indirect indicator for Z-ring formation[12,19]. Thus, we detected the effect of T0349 on the morphology of *M. smegmatis* by comparing the fluorescence of HADA on the strain in presence and absence of T0349. As is shown in Fig. 6A, in the absence of T0349, the septum located at the mid-cell. On addition of T0349, the typical morphology of *M. smegmatis* was shown. The length of the cells was significantly increased to induce the filamentation (Fig. 6B). As shown in Fig. 6F, the distribution of cell length was shown where 80% of the control cells were at the lower length range (< 5 μm), while the length of T0349 treated cells (>60%) was increased (5−10 μm). Importantly, the cells also changed by contracting at one end of the cells or forming the "bud" like structures (Fig. 6C−E). Many impaired septa appeared in a single cell treated with T0349, suggesting that T0349 disturbed formation and location of the functional Z-ring, and subsequently the cell division. Taken together, these results inferred that T0349 could likely inhibit the division of *M. smegmatis* by disturbing the location of Z-ring and formation of septum, which might be induced by blocking the interaction between FtsZ and SepF.

3.8. *Anti-Mtb activity of T0349*

FtsZ/SepF interaction is essential for the division of *M. tuberculosis* and disruption of the interaction will inhibit its proliferation. Therefore, we examined the anti-*Mtb* activity of T0349 against various *Mtb* strains. The first-line anti-TB drugs rifampin and isoniazid were used as controls. T0349 showed anti-*Mtb* activity with the MIC of 2 μg/mL against H37Rv (Table 1). For clinical sensitive strains (STB-FJ05349 and STB-FJ05060), the MICs of T0349 were both 1 μg/mL. T0349 also exhibited activity against multidrug-resistant *Mtb* strains MDR-FJ05120 and MDR-FJ05189 with the MICs of 2 μg/mL. For extensively drug resistant (XDR) clinical strain XDR-FJ05195, the MIC was 4 μg/mL. This indicated that T0349 had anti-*Mtb* activity comparable to the first-line anti-TB drugs.

Furthermore, we examined the activity of T0349 to other pathogens including *S. aureus, E. coli*, *K. pneumonia* and *P. aeruginosa*. Interestingly, T0349 showed high MICs (>32 μg/mL) on these strains, suggesting a high selectivity of this compound. SepF, the drug target of T0349, specific in *Mycobacteria* and absent in other strain, might result in the high selectivity of T0349.

In addition, the acute toxicity of T0349 was tested in ICR mice. The results showed that all mice survived for 7 days after single dose of T0349 ranging from 100 to 500 mg/kg. Meanwhile, compared with the saline (control) group, there was no change in body weight after treatment of T0349 (Fig. S6). It suggested that the approximate 50% lethal dose (LD_{50}) in mice was considered >500 mg/kg, indicating the safety of T0349 in mice.

4. Discussion

Bacteria cell division is a strictly mediated process that requires the coordination of multiple protein complex systems. Protein−protein interactions (PPIs) play essential role in this complex biological process. Therefore, targeting the key PPIs will be a promising strategy for anti-bacterial drug development. FtsZ, a bacterial cytoskeletal protein, interacts with many cell division proteins that modulate its ability to polymerize into the Z-ring and subsequently the Z-ring location[15,20]. SepF is one of the division proteins in *Mtb*[21]. The interaction of FtsZ and SepF proteins is critical for *M. tuberculosis* proliferation, thus compounds blocking FtsZ/SepF interaction will disturb the bacteria cell division. Here, we have established a yeast two-hybrid based inhibitor screening system targeted FtsZ/SepF interaction, from which we obtained compound T0349. As we know, most of the FtsZ inhibitors are discovered targeting the GTPase activity, the polymerization of FtsZ depending on[33,50]. Interestingly, compound T0349 reported in this research blocked the FtsZ/SepF interaction, leaving the GTPase of FtsZ unaffected. Using this screening system, we identified a compound T0349 with a distinctly different

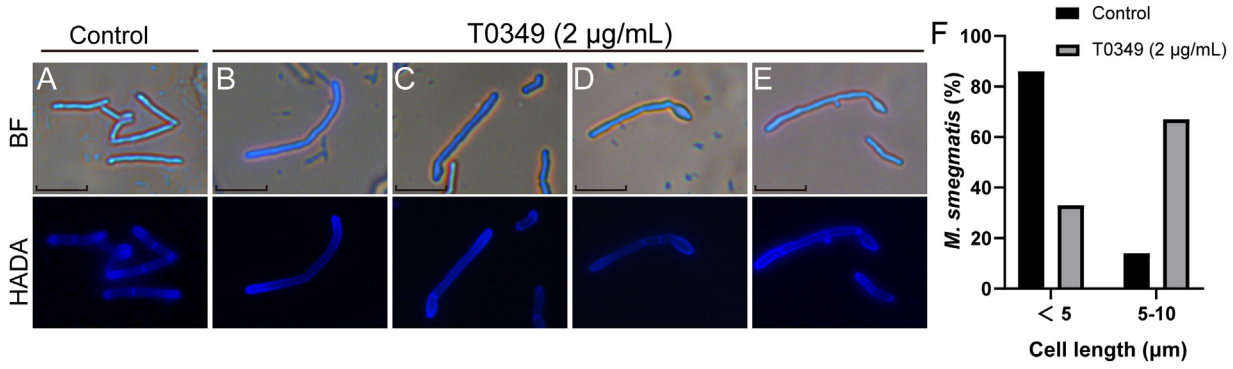

Figure 6 Representative microscopy images of *M. smegmatis* treated with T0349. *M. smegmatis* were incubated with 2 μg/mL T0349 (B−E), followed by stained with 0.5 mmol/L HADA. *M. smegmatis* strain without T0349 was used as a control (A). Bright field (BF) and HADA fluorescence images were shown. Scale bar, 3 μm. (F) The distribution of cell length for the control and T0349 treated *M. smegmatis* as measured by ImageJ. Three different visual fields were observed for each group and 50 bacterial cells were counted per field.

Table 1 MICs of T0349 against *Mtb* and various strains.

Strain	MIC (μg/mL)			
	T0349	Rifampin	Isoniazid	Levofloxacin
H37Rv	2	0.25	0.25	−
STB-FJ05349	1	0.5	0.5	−
STB-FJ05060	1	0.5	0.5	−
MDR-FJ05120	2	>256	4	−
MDR-FJ05189	2	>256	<0.5	−
XDR-FJ05195	4	4	>256	−
S. aureus 29213a	>32	−	−	0.25
S. aureus 33591b	>32	−	−	0.25
E. coli 25922c	>32	−	−	≤0.03
E. coli 09-1d	>32	−	−	4
K. pneumonia 700603d	>32	−	−	2
K. pneumonia 09-8c	>32	−	−	4
P. aeruginosa 27853	>32	−	−	4

STB, clinically sensitive strain of *Mtb*; MDR, multidrug-resistant *Mtb*; XDR, extensive drug-resistant *Mtb*; [a]MSSA; [b]MRSA; [c]ESBLs(−); [d]ESBLs(+).

mechanism to inhibit the polymerization of FtsZ and the Z-ring location. More importantly, T0349 showed anti-*Mtb* activity against various *Mtb* strains, while exhibiting no significant activity on other pathogens including *S. aureus, E. coli, K. pneumonia* and *P. aeruginosa.* This significant difference might be caused by the diverse division proteins interacting with FtsZ in different strains. SepF is a special interacting protein with FtsZ in *M. tuberculosis*, which is the alternative functional protein of MreB, FtsA and ZipA in other bacteria[19,20]. Therefore, the inhibitor of FtsZ/SepF interaction might have specific inhibition against *M. tuberculosis*.

Since compound T0349 inhibited FtsZ/SepF interaction, the cell division of *M. tuberculosis* treated with T0349 might be blocked. After adding T0349, the cells had filamentous morphology and abnormal septum. Some cells exhibited no septum due to the inhibition of FtsZ/SepF interaction by T0349, while some others showed septum located at the end of the elongated cells. As we know, there are some other FtsZ interacting proteins in *M. tuberculosis*, such as FhaB, ClpX and FtsW, which assists FtsZ polymerization to the Z-ring and subsequently the cell division together with SepF[19,51,52]. Thus, disruption of FtsZ/SepF interaction in cell could not completely inhibit the polymerization of FtsZ, resulting in the abnormal septum. However, SepF is essential for Z-ring location, which might be related to the mislocation of the abnormal septum. Interestingly, the morphology of *sepF* knockdown cell exhibited no septum in the elongated cell, inconsistent with the cells that the interaction of FtsZ/SepF was blocked. It is known that SepF interacts directly with MurG, a peptidoglycan-synthesizing enzyme essential for new septum synthesis in *Mycobacterium tuberculosiss*[20]. We speculated that the low expression of SepF might restrict the formation of septum, which can't be completely inhibited by blocking the interaction of FtsZ/SepF. The detailed mechanism needs to be clarified in the future.

In anti-TB drug discovery, both cell-based phenotypic screening and target-based biochemical screening have been proved very successful[53,54]. Most of the effective anti-TB compounds are obtained from these two complementary screening approaches[55,56]. However, the mechanisms of these compounds are not always immediately revealed. Therefore, identification of the drug target of these compounds has become critical and challenging. There are multiple approaches to uncover the drug target of the compounds, in which generating the gene mutant/knockout strains are the powerful tool to elucidate the mechanism of the anti-TB drug candidate. Traditional methods, such as inducible resistant mutants by antibiotics and homologous recombination technology, always take months to get a mutant strain and were not suitable for targeting essential genes[57,58]. A method for rapid gene modification, especially for essential genes is required. Recently, CRISPRi technology has been employed in drug discovery and target validation. It can be utilized to knockdown genes in a controllable way without changing the genome[46]. The knockdown strains with the under-expression of a drug target tend to make cells more sensitive to an on-target antibiotic. This strategy has been successfully applied to validate the drug target of rifampin and TB pipeline drug SQ109[59,60]. In this research, CRISPRi can achieve 99% knockdown of *ftsZ/sepF* gene expression in *M. smegmatis*. Drug susceptibility analysis of compound T0349 in *ftsZ/sepF* CRIPSRi strain further verified the results of SPR, FP and GST pulldown experiments. Although the application of CRISPRi as the rapid target validation for anti-TB drugs was not explored in this study, the described CRISPRi platform has provided a further target validation for the target-based biochemical screening. All these will accelerate the discovery of novel anti-TB agents.

Since the classic drug targets are usually enzymes, receptors and ion channels, PPIs involved in most biological processes are new potential drug targets[61−63]. Drugs that prevent the key PPIs could be valuable new therapeutic agents. However, the PPI inhibitors through small molecule compounds are generally considered difficult, for designing a small molecular to compete against the much larger interaction interface of PPI is challenging[61,64]. In fact, plenty of PPI inhibitors were applied into clinical trials, some of which have been successfully approved for use recently[61,65]. Indeed, PPI inhibitors can be modulated in a number of ways and is not limited by direct competing with protein−protein binding. Small molecular can also disrupt PPIs by allosteric destabilization or altering the dynamics of PPIs through binding with one protein[66]. In SPR experiment, the K_D for FtsZ/SepF interaction was 1−5 μmol/L, whereas the binding of T0349 to SepF was ∼50 μmol/L, indicating T0349 exhibited ∼10 folds lower affinity. We speculated that T0349 might disrupt FtsZ/SepF interaction through allosteric destabilization or altering the dynamics of the PPI by binding with SepF. Further investigation is needed to precisely explain the mechanism.

Compound T0349 was identified as a FtsZ/SepF interaction inhibitor of *M. tuberculosis* in this research. It is a naphthalene-based molecule, which has no bioactivity reported so far. Naphthalene scaffold is an important building block in drug discovery owning to its diverse biological activities through various structural modifications[67]. Large numbers of naphthalene derivatives have produced significant antibacterial activities in *E. coli*, *B. subtilis*, *S. aureus*, and *P. mirabilis*[68,69]. In anti-TB drug discovery, some naphthalene containing agents exhibited promising anti-TB activities[70,71]. Both bedaquiline and rifampin, widely used for TB treatment, were naphthalene-based molecules[72,73]. Thus, compound T0349 had the potential to be an ani-TB candidate. In our study, T0349 exhibited activity against drug-resistant *Mtb* strains with the MICs of 2−4 μg/mL, comparable to rifampin and isoniazid. However, many drug resistant *Mtb* strains are rifampin or isoniazid resistant. With that in mind, the anti-*Mtb* activity of T0349 was not fully satisfactory. Therefore, the structural modifications are needed to improve the activity of T0349.

5. Conclusions

In summary, we found that FtsZ/SepF interaction is a promising drug target in anti-TB drug discovery and we have identified a compound T0349 that inhibited bacterial cell division by disrupting FtsZ/SepF interaction. The mechanism of T0349 is significantly different from the classic GTPase inhibitors of FtsZ. In addition, T0349 has exhibited high selective antibacterial activities towards *M. tuberculosis*, making it a good candidate for anti-TB drug discovery. Although the activity of T0349 is suboptimal, we hope it could be optimized after structural modification. Therefore, FtsZ/SepF interaction appears to be a potential anti-TB drug target for identifying agents with novel mechanisms. Our results also demonstrate that CRISPRi technology could be a convenient tool in confirming drug target of anti-TB drugs.

Acknowledgments

This work was supported by CAMS Innovation Fund for Medical Sciences (CIFMS) (2021-I2M-1-026, 2022-I2M-2-002, 2021-I2M-JB-011, China) and National Natural Science Foundation of China (No. 81773784) and Beijing Key Laboratory of Non-Clinical Drug Metabolism and PK/PD study (Z1411020 04414062, China).

Author contributions

Jiandong Jiang, Shuyi Si and Yuan Lin planned and designed the study. Hongjuan Zhang, Ying Chen, Yu Zhang and Luyao Qiao carried out the experiment and collected the data. Hongjuan Zhang, Ying Chen and Xiangyin Chi analyzed the data. Yanxing Han provided technical support. Hongjuan Zhang, Yuan Lin, Shuyi Si and Jiandong Jiang wrote and revised the manuscript. All authors approved the final version of the manuscript.

Conflicts of interest

The authors declare no competing interests.

Appendix A. Supporting information

Supporting data to this article can be found online at https://doi.org/10.1016/j.apsb.2023.01.022.

References

1. Pai M, Behr MA, Dowdy D, Dheda K, Divangahi M, Boehme CC, et al. Tuberculosis. *Nat Rev Dis Prim* 2016;**2**:16076.
2. Ravimohan S, Kornfeld H, Weissman D, Bisson GP. Tuberculosis and lung damage: from epidemiology to pathophysiology. *Eur Respir Rev* 2018;**27**:170077.
3. WHO. *Global tuberculosis report 2021*. 2021. Accessed [May 20, 2022]. Available from: https://www.who.int/publications/i/item/9789240037021.
4. Bagcchi S. Dismal global tuberculosis situation due to COVID-19. *Lancet Infect Dis* 2021;**21**:1636.
5. González-Domenech CM, Pérez-Hernández I, Gómez-Ayerbe C, Viciana Ramos I, Palacios-Muñoz R, Santos J. A pandemic within other pandemics. when a multiple infection of a host occurs: SARS-CoV-2, HIV and *Mycobacterium tuberculosis*. *Viruses* 2021;**13**:931.
6. Peloquin CA, Davies GR. The Treatment of tuberculosis. *Clin Pharmacol Ther* 2021;**110**:1455−66.
7. Kadura S, King N, Nakhoul M, Zhu H, Theron G, Köser CU, et al. Systematic review of mutations associated with resistance to the new and repurposed *Mycobacterium tuberculosis* drugs bedaquiline, clofazimine, linezolid, delamanid and pretomanid. *J Antimicrob Chemother* 2020;**75**:2031−43.
8. Singh R, Dwivedi SP, Gaharwar US, Meena R, Rajamani P, Prasad T. Recent updates on drug resistance in *Mycobacterium tuberculosis*. *J Appl Microbiol* 2020;**128**:1547−67.
9. WHO. *Global tuberculosis report 2018*. 2018. Accessed [May 20, 2022]. Available from: https://apps.who.int/iris/bitstream/handle/10665/274453/9789241565646-eng.pd.
10. WHO. *WHO operational handbook on tuberculosis. Module 4: treatment−drug-resistant tuberculosis treatment*. 2020. Published [May 24, 2022]. Accessed [June 18, 2022]. Available from: https://www.who.int/publications/i/item/9789240006997.
11. Mahone CR, Goley ED. Bacterial cell division at a glance. *J Cell Sci* 2020;**133**:jcs237057.
12. Yang X, Lyu Z, Miguel A, McQuillen R, Huang KC, Xiao J. GTPase activity-coupled treadmilling of the bacterial tubulin FtsZ organizes septal cell wall synthesis. *Science* 2017;**355**:744−7.
13. Löwe J, Amos LA. Erratum to: prokaryotic cytoskeletons: filamentous protein polymers active in the cytoplasm of bacterial and archaeal cells. *Subcell Biochem* 2017;**84**:E1.
14. Fleurie A, Lesterlin C, Manuse S, Zhao C, Cluzel C, Lavergne JP, et al. MapZ marks the division sites and positions FtsZ rings in *Streptococcus pneumoniae*. *Nature* 2014;**516**:259−62.
15. Huang KH, Durand-Heredia J, Janakiraman A. FtsZ ring stability: of bundles, tubules, crosslinks, and curves. *J Bacteriol* 2013;**195**:1859−68.
16. Gamba P, Veening JW, Saunders NJ, Hamoen LW, Daniel RA. Two-step assembly dynamics of the *Bacillus subtilis* divisome. *J Bacteriol* 2009;**191**:4186−94.
17. Haeusser DP, Margolin W. Splitsville: structural and functional insights into the dynamic bacterial Z ring. *Nat Rev Microbiol* 2016;**14**:305−19.
18. Goehring NW, Beckwith J. Diverse paths to midcell: assembly of the bacterial cell division machinery. *Curr Biol* 2005;**15**:R514−26.
19. Kieser KJ, Rubin EJ. How sisters grow apart: mycobacterial growth and division. *Nat Rev Microbiol* 2014;**12**:550−62.
20. Gupta S, Banerjee SK, Chatterjee A, Sharma AK, Kundu M, Basu J. Essential protein SepF of mycobacteria interacts with FtsZ and

MurG to regulate cell growth and division. *Microbiology* 2015;**161**:1627−38.
21. Hamoen LW, Meile JC, de Jong W, Noirot P, Errington J. SepF, a novel FtsZ-interacting protein required for a late step in cell division. *Mol Microbiol* 2006;**59**:989−99.
22. Gola S, Munder T, Casonato S, Manganelli R, Vicente M. The essential role of SepF in mycobacterial division. *Mol Microbiol* 2015;**97**:560−76.
23. Slayden RA, Knudson DL, Belisle JT. Identification of cell cycle regulators in *Mycobacterium tuberculosis* by inhibition of septum formation and global transcriptional analysis. *Microbiology* 2006;**152**:1789−97.
24. White ML, Eswara PJ. *ylm* has more than a (Z anchor) ring to it!. *J Bacteriol* 2021;**203**:e004600-20.
25. Löwe J, Amos LA. Crystal structure of the bacterial cell-division protein FtsZ. *Nature* 1998;**391**:203−6.
26. Cendrowicz E, van Kessel SP, van Bezouwen LS, Kumar N, Boekema EJ, Scheffers DJ. *Bacillus subtilis* SepF binds to the C-terminus of FtsZ. *PLoS One* 2012;**7**:e43293.
27. Li X, Ma S. Advances in the discovery of novel antimicrobials targeting the assembly of bacterial cell division protein FtsZ. *Eur J Med Chem* 2015;**95**:1−15.
28. Yu HH, Kim KJ, Cha JD, Kim HK, Lee YE, Choi NY, et al. Antimicrobial activity of berberine alone and in combination with ampicillin or oxacillin against methicillin-resistant *Staphylococcus aureus*. *J Med Food* 2005;**8**:454−61.
29. Tripathy S, Sahu SK. FtsZ inhibitors as a new genera of antibacterial agents. *Bioorg Chem* 2019;**91**:103169.
30. Tian X, Wang P, Li T, Huang X, Guo W, Yang Y, et al. Self-assembled natural phytochemicals for synergistically antibacterial application from the enlightenment of traditional Chinese medicine combination. *Acta Pharm Sin B* 2020;**10**:1784−95.
31. Margalit DN, Romberg L, Mets RB, Hebert AM, Mitchison TJ, Kirschner MW, et al. Targeting cell division: small-molecule inhibitors of FtsZ GTPase perturb cytokinetic ring assembly and induce bacterial lethality. *Proc Natl Acad Sci U S A* 2004;**101**:11821−6.
32. Gentry EJ, Jampani HB, Keshavarz-Shokri A, Morton MD, Velde DV, Telikepalli H, et al. Antitubercular natural products: berberine from the roots of commercial *Hydrastis canadensis* powder. Isolation of inactive 8-oxotetrahydrothalifendine, canadine, beta-hydrastine, and two new quinic acid esters, hycandinic acid esters-1 and -2. *J Nat Prod* 1998;**61**:1187−93.
33. Lin Y, Zhang H, Zhu N, Wang X, Han Y, Chen M, et al. Identification of TB-E12 as a novel FtsZ inhibitor with anti-tuberculosis activity. *Tuberculosis* 2018;**110**:79−85.
34. Lin Y, Zhu N, Han Y, Jiang J, Si S. Identification of anti-tuberculosis agents that target the cell-division protein FtsZ. *J Antibiot* 2014;**67**:671−6.
35. Saeloh D, Wenzel M, Rungrotmongkol T, Hamoen LW, Tipmanee V, Voravuthikunchai SP. Effects of rhodomyrtone on Gram-positive bacterial tubulin homologue FtsZ. *PeerJ* 2017;**5**:e2962.
36. James P, Halladay J, Craig EA. Genomic libraries and a host strain designed for highly efficient two-hybrid selection in yeast. *Genetics* 1996;**144**:1425−36.
37. Lin Y, Li Y, Zhu Y, Zhang J, Li Y, Liu X, et al. Identification of antituberculosis agents that target ribosomal protein interactions using a yeast two-hybrid system. *Proc Natl Acad Sci U S A* 2012;**109**:17412−7.
38. Xiao J, Jia H, Pan L, Li Z, Lv L, Du B, et al. Application of the CRISPRi system to repress sepF expression in *Mycobacterium smegmatis*. *Infect Genet Evol* 2019;**72**:183−90.
39. Collins L, Franzblau SG. Microplate alamar blue assay *versus* BACTEC 460 system for high-throughput screening of compounds against *Mycobacterium tuberculosis* and *Mycobacterium avium*. *Antimicrob Agents Chemother* 1997;**41**:1004−9.
40. CLSI. *Performance standards for antimicrobial susceptibility testing, M100*. 30th ed. PA: Clinical Laboratory Standards Institute; 2020.
41. Duman R, Ishikawa S, Celik I, Strahl H, Ogasawara N, Troc P, et al. Structural and genetic analyses reveal the protein SepF as a new membrane anchor for the Z ring. *Proc Natl Acad Sci U S A* 2013;**110**:E4601−10.
42. Singh JK, Makde RD, Kumar V, Panda D. SepF increases the assembly and bundling of FtsZ polymers and stabilizes FtsZ protofilaments by binding along its length. *J Biol Chem* 2008;**283**:31116−24.
43. Gündoğdu ME, Kawai Y, Pavlendova N, Ogasawara N, Errington J, Scheffers DJ, et al. Large ring polymers align FtsZ polymers for normal septum formation. *EMBO J* 2011;**30**:617−26.
44. Yan G, Li D, Lin Y, Fu Z, Qi H, Liu X, et al. Development of a simple and miniaturized sandwich-like fluorescence polarization assay for rapid screening of SARS-CoV-2 main protease inhibitors. *Cell Biosci* 2021;**11**:199.
45. Löfås S. Biacore systems: leading the revolution in label-free interaction analysis. *Biointerphases* 2008;**3**:2−3.
46. Rock JM, Hopkins FF, Chavez A, Diallo M, Chase MR, Gerrick ER, et al. Programmable transcriptional repression in mycobacteria using an orthogonal CRISPR interference platform. *Nat Microbiol* 2017;**2**:16274.
47. Qi LS, Larson MH, Gilbert LA, Doudna JA, Weissman JS, Arkin AP, et al. Repurposing CRISPR as an RNA-guided platform for sequence-specific control of gene expression. *Cell* 2013;**152**:1173−83.
48. McNicholl BP, McGrath JW, Quinn JP. Development and application of a resazurin-based biomass activity test for activated sludge plant management. *Water Res* 2007;**41**:127−33.
49. Kuru E, Tekkam S, Hall E, Brun YV, Van Nieuwenhze MS. Synthesis of fluorescent D-amino acids and their use for probing peptidoglycan synthesis and bacterial growth *in situ*. *Nat Protoc* 2015;**10**:33−52.
50. Han H, Wang Z, Li T, Teng D, Mao R, Hao Y, et al. Recent progress of bacterial FtsZ inhibitors with a focus on peptides. *FEBS J* 2021;**288**:1091−106.
51. Sureka K, Hossain T, Mukherjee P, Chatterjee P, Datta P, Kundu M, et al. Novel role of phosphorylation-dependent interaction between FtsZ and FipA in mycobacterial cell division. *PLoS One* 2010;**5**:e8590.
52. Rajagopalan M, Maloney E, Dziadek J, Poplawska M, Lofton H, Chauhan A, et al. Genetic evidence that mycobacterial FtsZ and FtsW proteins interact, and colocalize to the division site in *Mycobacterium smegmatis*. *FEMS Microbiol Lett* 2005;**250**:9−17.
53. Altaf M, Miller CH, Bellows DS, O'Toole R. Evaluation of the *Mycobacterium smegmatis* and BCG models for the discovery of *Mycobacterium tuberculosis* inhibitors. *Tuberculosis* 2010;**90**:333−7.
54. Swinney DC. Phenotypic *vs*. target-based drug discovery for first-in-class medicines. *Clin Pharmacol Ther* 2013;**93**:299−301.
55. Dalberto PF, de Souza EV, Abbadi BL, Neves CE, Rambo RS, Ramos AS, et al. Handling the hurdles on the way to anti-tuberculosis drug development. *Front Chem* 2020;**8**:586294.
56. Bahuguna A, Rawat DS. An overview of new antitubercular drugs, drug candidates, and their targets. *Med Res Rev* 2020;**40**:263−92.
57. Kim JH, Wei JR, Wallach JB, Robbins RS, Rubin EJ, Schnappinger D. Protein inactivation in mycobacteria by controlled proteolysis and its application to deplete the beta subunit of RNA polymerase. *Nucleic Acids Res* 2011;**39**:2210−20.
58. Wei JR, Krishnamoorthy V, Murphy K, Kim JH, Schnappinger D, Alber T, et al. Depletion of antibiotic targets has widely varying effects on growth. *Proc Natl Acad Sci U S A* 2011;**108**:4176−81.
59. McNeil MB, Cook GM. Utilization of CRISPR interference to validate MmpL3 as a drug target in *Mycobacterium tuberculosis*. *Antimicrob Agents Chemother* 2019;**63**:e006299-19.
60. Faulkner V, Cox AA, Goh S, van Bohemen A, Gibson AJ, Liebster O, et al. Re-sensitization of *Mycobacterium smegmatis* to rifampicin using CRISPR interference demonstrates its utility for the study of non-essential drug resistance traits. *Front Microbiol* 2020;**11**:619427.

61. Lu H, Zhou Q, He J, Jiang Z, Peng C, Tong R, et al. Recent advances in the development of protein−protein interactions modulators: mechanisms and clinical trials. *Signal Transduct Target Ther* 2020;**5**:213.
62. Martino E, Chiarugi S, Margheriti F, Garau G. Mapping, structure and modulation of PPI. *Front Chem* 2021;**9**:718405.
63. Wang W, Liu C, Zhu N, Lin Y, Jiang J, Wang Y, et al. Identification of anti-Gram-negative bacteria agents targeting the interaction between ribosomal proteins L12 and L10. *Acta Pharm Sin B* 2018;**8**:772−83.
64. Cheng AC, Coleman RG, Smyth KT, Cao Q, Soulard P, Caffrey DR, et al. Structure-based maximal affinity model predicts small-molecule druggability. *Nat Biotechnol* 2007;**25**:71−5.
65. Ran X, Gestwicki JE. Inhibitors of protein−protein interactions (PPIs): an analysis of scaffold choices and buried surface area. *Curr Opin Chem Biol* 2018;**44**:75−86.
66. Fischer G, Rossmann M, Hyvönen M. Alternative modulation of protein−protein interactions by small molecules. *Curr Opin Biotechnol* 2015;**35**:78−85.
67. Makar S, Saha T, Singh SK. Naphthalene, a versatile platform in medicinal chemistry: sky-high perspective. *Eur J Med Chem* 2019; **161**:252−76.
68. Azarifar D, Shaebanzadeh M. Synthesis and characterization of new 3,5-dinaphthyl substituted 2-pyrazolines and study of their antimicrobial activity. *Molecules* 2002;**7**:885−95.
69. Chopra B, Dhingra AK, Kapoor RP, Parsad DN. Synthesis and antimicrobial activity of naphthylamine analogs having azetidinone and thiazolidinone moiety. *J Explor Res Pharmacol* 2017;**2**: 105−12.
70. Tran T, Saheba E, Arcerio AV, Chavez V, Li QY, Martinez LE, et al. Quinones as antimycobacterial agents. *Bioorg Med Chem* 2004;**12**: 4809−13.
71. Mital A, Negi VS, Ramachandran U. Synthesis and biological evaluation of naphthalene-1,4-dione derivatives as potent antimycobacterial agents. *Med Chem* 2008;**4**:492−7.
72. Worley MV, Estrada SJ. Bedaquiline: a novel antitubercular agent for the treatment of multidrug-resistant tuberculosis. *Pharmacotherapy* 2014;**34**:1187−97.
73. Reddy VM, Nadadhur G, Daneluzzi D, Dimova V, Gangadharam PR. Antimycobacterial activity of a new rifamycin derivative, 3-(4-cinnamylpiperazinyl iminomethyl) rifamycin SV (T9). *Antimicrob Agents Chemother* 1995;**39**:2320−4.